Research article

Ultrasonic properties of Ni–Fe–B₄C cermets produced by tube furnace sintering

Vildan Özkan Bilici [ID]

Afyon Kocatepe University, Faculty of Arts and Sciences, Department of Physics, 03200, Afyonkarahisar, Turkey

A B S T R A C T

B_4C–Fe–based cermets with various Ni concentrations were produced by tube furnace sintering using the powder metallurgy method. The prepared cermets were sintered at 1000 °C under the argon shroud. Ultrasonic properties such as ultrasonic wave velocities, ultrasonic longitudinal and shear attenuation values, Young's (elastic) modulus, and Poisson's ratio were determined by the pulse-echo method using 2 MHz and 4 MHz probes. The obtained ultrasonic properties were used to characterize the properties of the samples. It was observed that ultrasonic wave velocities and Young's modulus decreased with increasing Ni concentration. At the same time, ultrasonic attenuation values and Poisson ratio increased with increasing Ni concentration. According to the results, the amount of Ni has an effective role in the structure of the cermets.

© 2022 The Authors. Published by Synsint Research Group.

1. Introduction

Cermets are hard ceramic-metal composites with the dominant ceramic phases, and there are increasing applications of cermets used to produce materials with the best properties such as high hardness, wear resistance, corrosion-erosion resistance and resistance to high-temperature deformation [1–3]. Today, cermets are used in cutting and plotter tool bits, in the machine-building industry, in the medical and food industries, etc. used [4–6]. In order to understand the effect of enhanced high-temperature protection, grain formation and grain boundary on the strength and other properties of cermets, different methods are used to develop new types of cermets and to predict and investigate their properties. One of these techniques is the ultrasonic testing technique. Ultrasonic testing (UT) is one of the most widely used nondestructive testing (NDT) techniques for determining the properties of internal defects of various materials [7]. Ultrasonic NDT, a versatile technique capable of material analysis, is perhaps better known for its more common applications for thickness measurement, flaw detection and acoustic imaging, while high-frequency sound mechanical, structural or compositional properties of solids and liquids [8–10]. In the most widely used pulse-echo UT process, the received

signal of ultrasonic pulsed waves reflected through the material can be analyzed to obtain geometric parameters such as the position, size and orientation of the particles in the material [11, 12]. Boron carbide ceramics exhibit characteristic properties such as high hardness, high wear resistance, low density, high neutron absorbance in cross-section, durability at high temperatures and high chemical resistance. Therefore, B_4C, thanks to its superior physical and chemical properties, is used in the refractory industry, nuclear reactors, extrusion dies, metal matrix composites, solid missile fuels and as an abrasive [7–9]. Due to the very strong covalent bonds between boron and carbon atoms, boron carbide is a difficult compound to sinter. Additives such as C, Al, Fe, Ti, Si, Al_2O_3 and ZrO_2 are added to improve the sintering behavior and mechanical properties [13–15].

Powder Metallurgy (P/M) is a modern manufacturing method and is very suitable for the production of high-tech materials. When the production processes are considered in general terms, powder metallurgy is a method consisting of powder preparation, mixing, pressing and sintering steps to prepare metallic materials with a uniform microstructure without separating alloying elements [16–18]. The advantage of this method is that the sintering temperature is lower than the melting point, so the material can be produced at a low cost. In
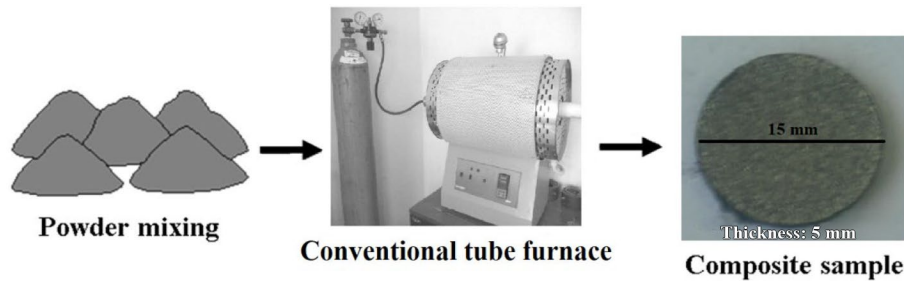
Fig. 1. Production process of metal-matrix component samples with powder metallurgy.

recent years, due to the need for light and superior materials, the application of powder metallurgy technology has increased due to the new development of technology in the aviation, space and automotive sectors [19, 20].

In this study, nickel was used as the additive material and B_4C-Fe based Ni cermets were obtained by using powder metallurgy method. SEM techniques were used to characterize the microstructures formed during the sintering process. At the same time, ultrasonic measurements were taken using the ultrasonic pulse-echo method for measurements that depend on the structure of the sample without damaging the sample. Ultrasonic attenuation, velocity and related parameters provide an understanding of the micro-structural and physical properties of the material and its internal structure.

2. Materials and method

2.1. Experimental details

In this study, 12.5% Ni–37.5% Fe–50% B_4C, 25% Ni–25% Fe–50% B_4C and 37.5% Ni–12.5% Fe–50% B_4C samples were produced in volumetric varying compositions. Metallic powders used in the study were Ni powders with 99.8% purity and -325 mesh particle size from Alfa Aesar, Fe powders with 97% purity and -325 mesh particle size, and boron carbide powder with 98% purity and -200 mesh particle size. Both powders were supplied from Sigma Aldrich company. The composition of the powder samples (Ni–Fe–B_4C) was prepared in 5 g cylindrical compressed pre-form. The chemical powders to be used for the production of cermets were first mixed mechanically in the blender. The powders prepared in the determined amounts were mixed in the mixer rotating at 20 dv/dk speed for 24 hours in order to obtain a homogeneous mixture. Then, all the powders were placed in a steel

mold with a diameter of 15 mm and a height of 5 mm and pressed in a hydraulic press at a pressure of 305.9 kg/cm^2, then the cold-pressed samples underwent sintering at 1000 °C for 2 hours in a traditional tube furnace using Argon gas atmosphere (Fig. 1). While the sintering process is initiated at room temperature, the temperature rise is approximately 10 °C per minute. Because the temperature rise during sintering is slow, any reaction that may occur in the sample with temperature occurs slowly and reliably, events such as cracking, breaking, and dispersion doesn't occurs, and at the same time, the sintered surface is smooth. Thus, the samples were made ready for physical-ultrasonic analyses. SEM images of sintered Ni–Fe–B_4C samples are shown in Fig. 2.

2.2. Ultrasonic analysis

Destructive, semi-destructive and non-destructive testing (NDT) techniques are available for full characterization. Ultrasonic testing parameters are significantly affected by changes in the microstructural or mechanical properties of materials.

Ultrasonic measurement systems are designed to produce the necessary energy for the propagation of ultrasonic waves in solid, liquid and gas environments, and to measure propagation velocities, damping factors or energy losses in ultrasonic environments. In ultrasonic measurement methods, as in every experimental system, there is a transducer that produces the sound wave and another transducer that detects the produced sound wave from the other end of the environment (Fig. 3). Pulse echo method, which is one of the most preferred ultrasonic measurement methods for the characterization of material properties, was used in the study. Ultrasonic pulse-echo technique is generally used to take precise ultrasonic velocity and attenuation measurements in the megahertz and gigahertz frequency regions, to evaluate elastic
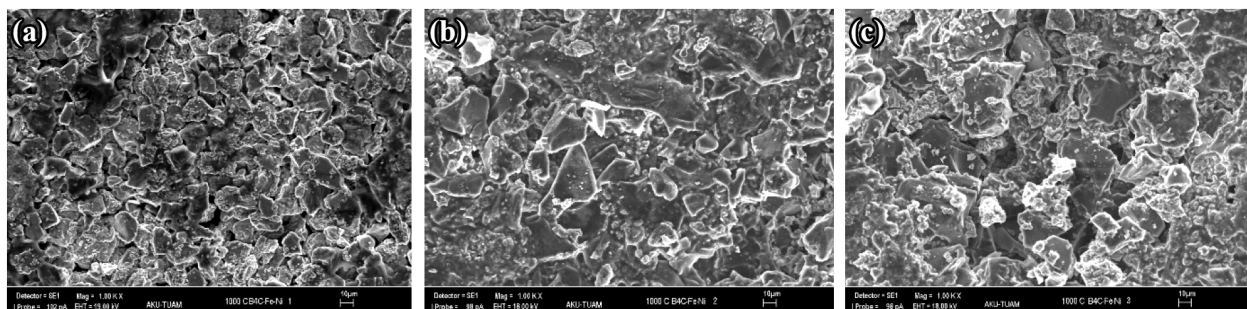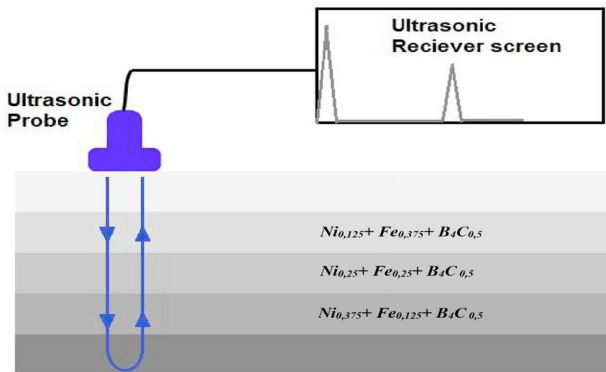

Fig. 2. SEM images of a) 12.5% Ni–37.5% Fe–50% B_4C, b) 25% Ni–25% Fe–50% B_4C, and c) 37.5% Ni–12.5% Fe–50% B_4C cermet samples.

Fig. 3. Schematic of Ni-Fe-B$_4$C composition and the pulse-echo ultrasonic test arrangement.

modulus of materials, to determine microstructure characterization and to evaluate its mechanical property [21, 22]. Velocity and attenuation measurements of the samples were made with Sonatest Sitescan 150 model ultrasonic wave flaw detector. 2 MHz (Sonatest SLH2-10) transmitter/receiver longitudinal probe was used to measure ultrasonic longitudinal velocity and 4 MHz (GE Inspection Technologies MB 4Y 66100541) transmitter/receiver shear probe was used to measure ultrasonic shear wave velocity. Sonatest sonagel-W liquid gel was used as a coupling fluid between the probes and the sample. Then, the image of the ultrasonic wave sent to the sample with the transmitter/receiver transducer was obtained with the front wall reflection, back wall reflection peaks and echoes peaks on the A-Scan screen. By changing the height of the transducers from the sample, measurements were made until the sharpest peak in the spectrum was obtained. The velocity of ultrasonic waves in the samples is calculated as follows:

$$V = \frac{2d}{t} \tag{1}$$

where d: sample thickness (mm), t: propagation time of ultrasonic wave (ns) and V: propagation speed of ultrasonic wave (m/s) [23–25]. Assuming the samples used in this analysis are isotropic, standard rate-elasticity formulas can be used to calculate the Young's modulus if the density of the sample is known. These formulas are:

$$E = \rho V_T^2 \frac{3V_L^2 - 4V_T^2}{V_L^2 - V_T^2} \tag{2}$$

$$\nu = \frac{V_L^2 - 2V_T^2}{2V_L^2 - 2V_T^2} \tag{3}$$

E, ν, and ρ values are Young's (elastic) modulus, Poisson's ratio and density of the sample, respectively [26, 27]. The attenuation term is used for the average energy loss that occurs due to the one-to-one interaction with the particles in the medium while the ultrasonic wave propagates in a solid medium. This reduction event occurs due to the absorption and scattering properties of the solid and is called "attenuation". Attenuation refers to the loss of signal amplitude with increasing propagation distance. Loss is defined as the ratio of two amplitudes and is expressed in logarithmic units Neper or dB with amplitude [28, 29]. The attenuation coefficient was calculated by the ratio of the amplitudes of two consecutively reflected ultrasonic waves.

$$\alpha = \frac{1}{d} 20 \log \frac{A_1}{A_2} \tag{4}$$

3. Results and discussion

The scope of this study is to investigate the ultrasonic properties of Ni-Fe-B$_4$C cermets. Ultrasonic velocity measurements were made in cermets produced by the powder metallurgy method, and the effect of Ni concentrations at different rates on the elastic modulus and Poisson ratio was also examined. The measurement results of the ultrasonic longitudinal wave velocities, ultrasonic shear wave velocities, longitudinal and shear attenuation values, Young's modulus and Poisson's ratio of Ni-Fe-B$_4$C cermets sintered with different nickel concentrations are shown in Table 1. In addition, the density values of the cermets after sintering were determined by Archimedes method and are shown in Table 1.

Longitudinal and shear wave velocities, attenuation values, elasticity (Young's) modulus and Poisson ratios of 12.5% Ni/Fe/B$_4$C, 25% Ni/Fe/B$_4$C and 37.5% Ni/Fe/B$_4$C cermets prepared in different ratios were investigated. When looking at the table, graphs were drawn depending on the nickel concentration in order to understand the difference between them and whether their interactions are significant or not. Looking at the graphs, it is seen that the change depending on the nickel concentration is effective in the cermet structure to be formed, and the ultrasonic longitudinal and shear wave velocity decreases with its increase (Fig. 4a). It also appears that ultrasonic attenuation increases against increasing percentage rates (Fig. 4b). One of the most important factors affecting ultrasound wave speed is porosity. Therefore, SEM analyze were performed on the samples to reveal the effect of Ni concentration doped at different rates and to characterize the changes occurring in the sample (Fig. 2).

As a result of the full wetting and bonding of the nickel powder particles, it is observed that the porous structure is formed despite the grain coarsening and a decrease in the total volume. There are also pores that exhibit homogeneous distribution between particles. Since the B$_4$C preform produced by nickel doping has a porous morphology, the sound wave sent into the structure is strongly reflected from the

Table 1. Ultrasonic longitudinal and shear velocity, longitudinal attenuation and shear attenuation, Young's (elastic) modulus, Poisson's ratio and density values of cermets.

Sample	V_L (m/s)	V_T (m/s)	Longitudinal attenuation (dB/mm)	Shear attenuation (dB/mm)	E (GPa)	Poisson's ratio	Density (g/cm^3)
Ni$_{0,125}$ + Fe$_{0,375}$ + B$_4$C$_{0,5}$	2611	1883	1.059	1.517	17.67	-0.01	2.6
Ni$_{0,25}$ + Fe$_{0,25}$ + B$_4$C$_{0,5}$	2573	1806	1.279	1.609	17.19	0.01	2.6
Ni$_{0,375}$ + Fe$_{0,125}$ + B$_4$C$_{0,5}$	2383	1659	1.354	1.625	14.70	0.03	2.6
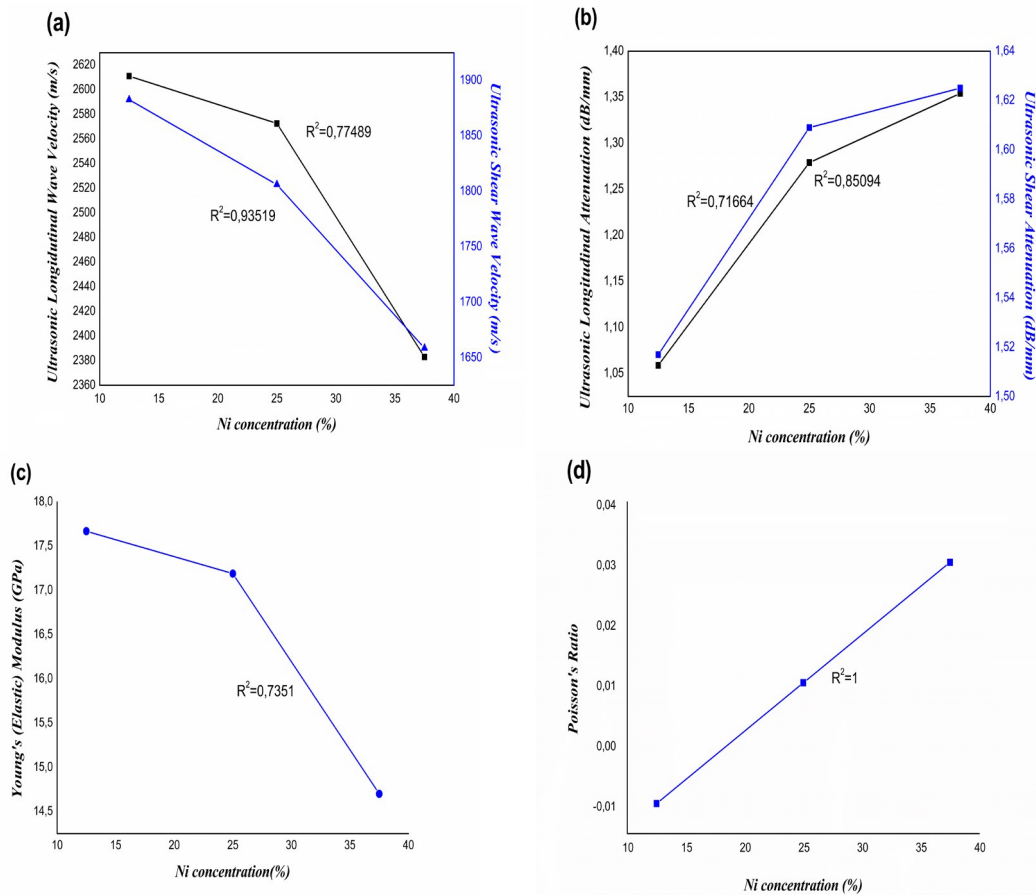
Fig. 4. The relationship between a) ultrasonic velocities-nickel concentration (%), b) ultrasonic attenuation-nickel concentration (%), c) Young's (Elastic) modulus-nickel concentration (%), and d) Poisson's ratio-nickel concentration (%) of Ni-Fe-B₄C cermet.

interfaces. Cracks, thin layer accumulations, shrinkage, pits, voids, porous parts and structures that disrupt the continuity of the internal structure will cause a loss in the ultrasonic sound wave entering the structure because they form interfaces. Therefore, it is seen as a decrease in the results obtained. Absorption of ultrasonic sound waves by the discontinuities encountered in the structure also causes an increase in ultrasonic attenuation values. Young's (elasticity) modulus and Poisson's ratio increase linearly depending on nickel concentration (Fig. 4c and Fig. 4d). Elastic properties of solids Young's modulus; is explained by flexibility in length. Accordingly, it is possible for the shape or size of an object to change under the influence of any external force. A decrease in Young's modulus means that the flexibility of the structure decreases, which means that the structure is porous and brittle. It is seen that the nickel concentration increases linearly with the Poisson ratio. Even the correlation coefficient is $R^2 = 1$. When the correlation coefficient approaches 0, it indicates the existence of a weak relationship between the variables. When the correlation coefficient is examined in the graphics, it is clearly seen that the analyzed analyzes are related to each other. Poisson's ratio is the mathematical value of how many a material contract or expands under pressure. This value is directly related to the main mechanical properties of the material. While most known materials have a positive Poisson ratio, there are a few negative Poisson ratios, also known as "Auxetic" materials. Also, it is known that the Poisson ratio certainly does not exceed 0.5 [30].

4. Conclusions

In the study, the ultrasonic technique was used effectively for the characterization of Ni-Fe-B₄C cermet properties produced by the powder metallurgy method in different compositions. Ultrasonic properties of the samples were investigated depending on the amount of sintered nickel at different rates. Young's (elasticity) modulus and Poisson's ratio are all positive and interdependent with the results obtained. The physical-ultrasonic properties of Ni-Fe-B₄C cermet samples were evaluated using the pulse-echo method, which is one of the non-destructive testing methods. Looking at the graphics in general;

- In the measurements and graphics, it has been determined that the propagation velocity (shear and longitudinal) and Young's (elasticity) modulus values of ultrasonic waves inversely vary with the amount of nickel.
- At the same time, the attenuation values and the Poisson's ratio show a directly proportional change with the nickel amount. Since boron carbide has a porous and brittle structure, even though it is sintered with nickel reinforcement, the low closed pore amount remains constant with the self-regulation of the grains.
- Accordingly, since the ultrasonic wave is lost in the pore in the structure, that is, the absorption process increases, and the ultrasonic wave velocity will decrease. B₄C exhibits brittle fracture and constitutes linear deformation at low stresses.

References

[1] A. Abramovich, Ultrasonic investigations of cermets elastic properties in dependence on steel concentration and temperature of sintering, IOP Conf. Series: Mater. Sci. Eng. 42 (2012) 1–4. https://doi:10.1088/1757-899X/42/1/012027.

[2] B. Rogé, J.S.R. Giguère, K.I. McRae, A. Fahr, Nondestructive evaluation of a cermet coating using ultrasonic and eddy current techniques, AIP Conf. Proc. 615 (2002) 1201–1208. https://doi.org/10.1063/1.1472931.

[3] K.T. Rarnesh, G. Ravichandran, An ultrasonic evaluation of damage in cermets, Review of Progress in Quantitative Nondestructive Evaluation. Springer, Boston, MA. (1989) 1841–1846. https://doi.org/10.1007/978-1-4613-0817-1_233.

[4] M.S. Alam, A.K. Das, Advancement in cermet-based coating on steel substrate: A review, Mater. Today: Proc. (2022) 805–810. https://doi.org/10.1016/j.matpr.2022.02.260.

[5] S. Buchholz, Z.N. Farhat, G.J. Kipouros, K.P. Plucknett, The reciprocating wear behaviour of TiC–Ni3Al cermets, Int. J. Refract. Met. Hard Mater. 33 (2012) 44–52. https://doi.org/10.1016/j.ijrmhm.2012.02.008.

[6] L. Jaworska, M. Rozmus, B. Królicka, A. Twardowska, Functionally graded cermets, J. Achieve. Mater. Manuf. Eng. 17 (2006) 73–76.

[7] P. Khalili, P. Cawley, The choice of ultrasonic inspection method for the detection of corrosion at inaccessible locations, NDT E Int. 99 (2018) 80–92. https://doi.org/10.1016/j.ndteint.2018.06.003.

[8] G.K. Sun, Z.G. Zhou, Ultrasonic imaging of particle distribution in SiCp/Al composites, Mater. Testing. 59 (2017) 166–171. https://doi.org/10.3139/120.110985.

[9] A. Bhaskar, Characterization of hollow particulate and graded composites using ultrasonic technique, Master's Theses, University of Rhode Island. (2011). https://doi.org/10.23860/thesis-ale-bhaskar-2011.

[10] M. Toozandehjani, F. Ostovan, M. Shamshirsaz, K.A. Matori, E. Shafiei, Velocity and attenuation of ultrasonic wave in Al/Al2O3 nanocomposite and their correlation to microstructural evolution during synthesizing procedure, J. Mater. Res. Technol. 15 (2021) 2529–2542. https://doi.org/10.1016/j.jmrt.2021.09.065.

[11] V. Özkan, İ.H. Sarpün, A. Erol, A. Yönetken, Influence of mean grain size with ultrasonic velocity on micro-hardness of B4C–Fe–Ni composite, J. Alloys Compd. 574 (2013) 512–519. https://doi.org/10.1016/j.jallcom.2013.05.097.

[12] M. Toozandehjani, K.A. Matori, F. Ostovan, F. Mustapha, N.I. Zahari, A. Oskoueian, On the correlation between microstructural evolution and ultrasonic properties: A review, J. Mater. Sci. 50 (2015) 2643–2665. https://doi.org/10.1007/s10853-015-8855-x.

[13] F. Thevenot, Boron carbide-A comprehensive review, J. Eur. Ceram. Soc. 6 (1990) 205–225. https://doi.org/10.1016/0955-2219(90)90048-K.

[14] O. Conde, A.J. Silvestre, J.C. Oliveira, Influence of carbon content on the crystallographic structure of boron carbide films, Surf. Coat. Technol. 125 (2000) 141–146. https://doi.org/10.1016/S0257-8972(99)00594-0.

[15] S. Koç, B. Akçay, B4C ve Al2O3 Seramik Plakaların Mekanik ve Balistik Özelliklerinin İncelenmesi, J. Polytechnic 1 (2021) 1–9. https://doi.org/10.2339/politeknik.801714.

[16] G.T. Sudha, B. Stalin, M. Ravichandran, M. Balasubramanian, Mechanical properties, characterization and wear behavior of powder metallurgy composites-A Review, Mater. Today: Proc. 22 (2020) 2582–2596. https://doi.org/10.1016/j.matpr.2020.03.389.

[17] A.M. Sankhla, K.M. Patel, M.A. Makhesana, K. Giasin, D.Y. Pimenov, et al., Effect of mixing method and particle size on hardness and compressive strength of aluminium based metal matrix composite prepared through powder metallurgy route, J. Mater. Res. Technol. 18 (2022) 282–292. https://doi.org/10.1016/j.jmrt.2022.02.094.

[18] S.K. Sharma, K.K. Saxena, K.B. Kumar, N. Kumar, The effect of reinforcements on the mechanical properties of AZ31 composites prepared by powder metallurgy: An overview, Mater. Today: Proc. (2021) 1–7. https://doi.org/10.1016/j.matpr.2021.11.639.

[19] G. Manohar, K.M. Pandey, S.R. Maity, Characterization of Boron Carbide (B4C) particle reinforced aluminium metal matrix composites fabricated by powder metallurgy techniques – A review, Mater. Today: Proc. 45 (2021) 6882–6888. https://doi.org/10.1016/j.matpr.2020.12.1087.

[20] A. Shamsipoor, B. Mousavi, M.S. Shaker, Synthesis and sintering of Fe-32Mn-6Si shape memory alloys prepared by mechanical alloying, Synth. Sinter. 2 (2022) 1–8. https://doi.org/10.53063/synsint.2022.2185.

[21] S. Lu, X. Wang, L. Teng, J. Zhang, Z. Zhou, et al., Finite element analysis and experimental investigation of ultrasonic testing of internal defects in SiCp/Al composites, Ceram. Int. 48 (2022) 5972–5982. https://doi.org/10.1016/j.ceramint.2021.11.133.

[22] A.P. Mouritz, C. Townsend, M.Z. Shah Khan, Non-destructive detection of fatigue damage in thick composites by pulse-echo ultrasonics, Compos. Sci. Technol. 60 (2000) 23–32. https://doi.org/10.1016/S0266-3538(99)00094-9.

[23] E.E. Gültekin., The effect of heating rate and sintering temperature on the elastic modulus of porcelain tiles, Ultrasonics. 83 (2018) 120–125. https://doi.org/10.1016/j.ultras.2017.06.005.

[24] S.Z. Khan, T.M. Khan, Y.F. Joya, M.A. Khan, S. Ahmed, A. Shah, Assessment of material properties of AISI 316L stainless steel using non-destructive testing, Nondestruct. Test. Eval. 31 (2016) 360–370. https://doi.org/10.1080/10589759.2015.1121265.

[25] F. Uzun, A.N. Bilge, Application of ultrasonic waves in measurement of hardness of welded carbon steels, Def. Technol. 11 (2015) 255–261. https://doi.org/10.1016/j.dt.2015.05.002.

[26] S.F. Farahmand, M.H. Soorgee, A.H. Monazzah, Evaluating the elastic properties of Al2O3–Al FGMs by longitudinal and transverse ultrasonic bulk waves velocity features, Ceram. Int. 47 (2021) 24906–24915. https://doi.org/10.1016/j.ceramint.2021.05.217.

[27] D.K. Pandey, S. Pandey, Ultrasonics: A technique of material characterization, Acoustic Waves, IntechOpen. (2010) 466. https://doi.org/10.5772/10153.

[28] N. Jai, M.-x. Su, X.-s. Cai, Particle size distribution measurement based on ultrasonic attenuation spectra using burst superposed wave, Results Phys. 13 (2019) 102273. https://doi.org/10.1016/j.rinp.2019.102273.

[29] M. Ramaniraka, S. Rakotonarivo, C. Payan, V. Garnier, Effect of the Interfacial Transition Zone on ultrasonic wave attenuation and velocity in concrete, Cem. Concr. Res. 124 (2019) 105809. https://doi.org/10.1016/j.cemconres.2019.105809.

[30] M. Ashjari, S.S. Hashemi, A. Rasoulian, Auxetic materials materials with negative Poisson's ratio, Mater. Sci. Eng. Int. J. 1 (2017) 62–64. https://doi.org/10.15406/mseij.2017.01.00011.